Fluorescence quantum efficiency and Auger upconversion losses of the stoichiometric laser crystal $NdAl_3(BO_3)_4$

C. Jacinto* and T. Catunda
Instituto de Física de São Carlos, Universidade de São Paulo–USP, CEP 13560-970, São Carlos, SP, Brazil

D. Jaque and J. García Solé
Departamento de Física de Materiales, Facultad de Ciencias, Universidad Autónoma de Madrid, Cantoblanco, 28049 Madrid, Spain
(Received 8 July 2005; published 13 December 2005)

Multiwavelength thermal lens technique has been carried out to determine the fluorescence quantum efficiency of Nd^{3+} ions in the $NdAl_3(BO_3)_4$ stoichiometric microchip laser crystal. The value obtained for the quantum efficiency, around 0.30, is an anomalously high value when compared with other Nd^{3+} stoichiometric crystals. Other parameters of great relevance in the laser performance (such as thermal diffusivity, thermal conductivity, and temperature induced path length change) have been also estimated. From the analysis of thermal lens measurements under different excitation intensities we have obtained the upconversion parameter. By comparing this experimental value with that calculated from the microscopic theory we have been able to determine the energy migration assisted upconversion as the dominant mechanism, in the excitation power regime used. Finally, we have concluded that energy transfer upconversion processes strongly reduce the metastable quantum efficiency constituting a non-negligible heat source in strongly pumped $NdAl_3(BO_3)_4$ crystals.

DOI: 10.1103/PhysRevB.72.235111 PACS number(s): 78.20.Nv, 78.55.−m, 78.90.+t, 78.60.−b

I. INTRODUCTION

Highly concentrated Nd^{3+} doped laser crystals are currently focusing much attention in the fields of solid state physics and lasers. From the fundamental point of view they open the possibility to study the basic physics taking place in highly dense media. As a matter of fact, some dynamical processes related to strong interactions between optically active ions are only accessible in these media in which average ion-ion distance is strongly reduced. As an example, the mechanisms leading to ion-ion energy exchange, and not only its efficiency, could be completely different in diluted and highly dense Nd^{3+} doped media. From the applied point of view, these highly concentrated Nd^{3+} doped laser crystals show strong absorption of pump radiation. Therefore, gain elements with typical dimensions of few hundreds of microns achieve enough gain to ensure efficient microchip laser oscillation.[1] Microchip geometry is of great interest in the development of compact laser sources for industry and communications and also is the basis of short and ultrashort laser pulse generation.[2]

However, for the majority of Nd^{3+} doped laser crystals, such as Nd:YAG and $Nd:YVO_4$, when the neodymium concentration is increased above a certain concentration their optical quality decreases and luminescence quenching is activated ($\sim$2 at. % in Nd:YAG),[3] leading to a strongly decrease in the metastable state fluorescence lifetime and quantum efficiency and, therefore, to a deterioration in the laser performance.[4,5] An interesting alternative is constituted by the so-called "self-activated crystals" (SACs). In these crystals, the Nd^{3+} ions are constituent of the lattice, and so concentrations as high as 5×10^{21} ions/cm^3 are achieved. These high concentrations provide efficient pump absorption in laser elements of reduced dimensions (less than 300 μm). Since Nd^{3+} ions constitute the crystalline lattice, these high ion concentrations are reached without any reduction in the optical quality of laser element.

Among of the great number of SACs crystals [such as $K_5Nd(MO_4)_4$,[6] Nd:LSB,[7,8] and Nd_3BWO_9 (Ref. 9)], neodymium aluminum borate, $NdAl_3(BO_3)_4$ (NAB) is of special relevance because its crystal structure provides nonvanishing electro optical coefficient allowing, for example, for monolithic integration of a miniature laser with a modulator in order to obtain an optical transmitter.[10] Highly efficient continuous wave infrared laser oscillation as well as short laser pulse generation have been already demonstrated from a microchip NAB laser cavities.[11,12] Recent works have pointed out that the microchip NAB laser performance is limited by the strong pump induced crystal heating, leading to non-negligible thermal effects inside the laser cavity.[11] Therefore, in order to develop an efficient NAB microchip laser a deep knowledge of its thermal properties (including thermal diffusivity and thermal conductivity) becomes necessary. Furthermore, due to the high Nd^{3+} concentration inside the crystal, second order excitation processes that populate the energy states higher than the metastable $^4F_{3/2}$ state could play an important role in the laser dynamics.[13,14] This aspect has been not taken previously into account although they can increase drastically the portion of pump radiation delivered to the lattice as heat.

In the particular case of NAB, it has been already demonstrated that the high energy levels are populated via an energy transfer upconversion (ETU) process.[15] This process involves the interaction of two excited closed Nd^{3+} ions in the $^4F_{3/2}$ metastable laser level, such that one ion relax to the $^4I_{11/2}$ and/or $^4I_{13/2}$ states while the other is promoted to a higher-lying excited state ($^4G_{7/2}$, $^2K_{13/2}$, $^4G_{9/2}$, $^2D_{3/2}$, $^4G_{11/2}$, or $^2K_{15/2}$). These states are depopulated by fast multiphonon relaxation back to the $^4F_{3/2}$ state, generating heat. In this way, the knowledge of the ETU processes related to these

transitions are necessary for the description of the nonradiative losses from the $^4F_{3/2}$ level as well as for the description of the pump induced thermal loading in NAB. Therefore, an accurate knowledge of the ETU rate (not accessible from conventional continuous wave optical spectroscopy) is also important for an appropriate design of strongly pumped NAB systems.

In this work we have used thermal lens (TL) spectrometry to determine the main thermal properties of NAB crystals, including thermal diffusivity (D), thermal conductivity (K), and the temperature coefficient of the optical path length (ds/dT).[16–18] It should be noticed that the quantity ds/dT is normalized by the sample length L, so that calling S_{opt} the sample optical path, $ds/dT=L^{-1}dS_{opt}/dT$.[17,18] In addition, the multiwavelength TL technique has been applied to determine the $^4F_{3/2}$ quantum efficiency as well as the ETU parameter and its effect on the metastable quantum efficiency without the need of the fluorescence kinetics. The ETU parameter obtained experimentally by the TL technique jointly with that calculated from the spectral properties of Nd^{3+} ions in NAB has been used to elucidate the dominant mechanism contributing to ETU. To the best of our knowledge this is the first time that the upconversion parameter, as well as the main mechanism responsible of it, are determined for the NAB crystal.

II. THEORETICAL BACKGROUND AND EXPERIMENTAL PROCEDURE

A. Pump induced thermal lensing

The TL effect is a well known phenomenon which takes place in nonhomogeneously pumped crystals (diode end pumped solid state laser, for example). It is caused by the deposition of heat into crystal lattice via the nonradiative decay processes taking place after the pump laser beam has been absorbed by the sample. Since pump intensity is not homogeneous, the pumping rate and, therefore, the amount of heat generated, follows an inhomogeneous spatial distribution inside the crystal. In this situation a transverse temperature gradient is established, and owing to the temperature dependence of refractive index, dn/dT, a refractive index gradient is produced, creating a lenslike optical element, the so-called TL. The propagation of a probe laser beam through this pump induced TL results in a variation of its on-axis intensity with respect to the unpumped crystal. If pump is suddenly switched on, then the on-axis intensity of the probe beam varies with time until it reaches a steady value. In this "*transient regime*," an analytical expression can be obtained for the time dependence of the probe beam on-axis intensity, which is given by[16–19]

$$\frac{I(t)}{I(0)}=\left\{1-\frac{\theta}{2}\tan^{-1}\left[\frac{2mV}{[(1+2m)^2+V^2]t_c/2t+1+2m+V^2}\right]\right\}^2, \tag{1}$$

where

(i) $I(t)$ is the on-axis probe beam intensity after a time t.

(ii) $I(0)$ the on-axis probe beam intensity just before pump beam is switched on, i.e., at $t=0$.

(iii) m the ratio between the probe and pump beam areas inside the crystal. Thus $m=(w_p/w_e)^2$, w_p and w_e being the probe and pump beam radii at the sample position, respectively.

(iv) V is defined as $V=Z_1/Z_c$ (when $Z_c \ll Z_2$) being Z_c the confocal distance of the probe beam, Z_1 the distance between the probe beam waist and the sample, and Z_2 the distance between the sample and the photodiode used to measure the time dependence of the on-axis probe beam intensity.

(v) t_c is the characteristic TL time, which is related to the thermal diffusivity, D, by $t_c=w_e^2/4D$. The thermal diffusivity can be expressed in terms of the thermal conductivity K as $D=K/\rho\cdot c$, where ρ is the density and c is the specific heat.

(vi) θ is basically the probe beam phase shift induced by the thermal lens.

From previous works it is known that the thermal lens induced phase shift is given by[16–19]

$$\theta=-P_{abs}\frac{1}{K\lambda_p}\left(\frac{ds}{dT}\right)_p\varphi, \tag{2}$$

where λ_p is the probe beam wavelength, P_{abs} the absorbed pump power, ds/dT the temperature coefficient of the optical path length, and φ is the fraction of absorbed energy converted into heat. This fraction is also known as absolute nonradiative quantum efficiency or fractional thermal loading. In fluorescent samples, like Nd^{3+} doped laser crystals, part of the absorbed excitation photon energy (hc/λ_{exc}) is converted into heat and part is converted in fluorescence, generating a photon with an average energy $hc/\langle\lambda_{em}\rangle$. Indeed this description is close to the real situation only when low pump powers are being absorbed by the sample. In this way cooperative excitations from the metastable state are negligible and so the only heat source is the nonradiative deexcitations from the metastable state. In this situation the fractional thermal loading is given by[20]

$$\varphi=1-\eta_0\frac{\lambda_{exc}}{\langle\lambda_{em}\rangle}, \tag{3}$$

where η_0 is the intrinsic metastable state ($^4F_{3/2}$) quantum efficiency. This efficiency is defined as the ratio of the number of radiative deexcitations to the total number of deexcitations taking place from the $^4F_{3/2}$ metastable state in the low intensity pumping range (i.e., in the absence of upconversion processes). Taking into account (3), the probe beam phase shift induced by the thermal lens [expression (2)] can be written in terms of metastable quantum efficiency as follows:

$$\theta=-P_{abs}\frac{1}{K\lambda_p}\left(\frac{ds}{dT}\right)_p\left(1-\eta_0\frac{\lambda_{exc}}{\langle\lambda_{em}\rangle}\right). \tag{4}$$

When working with TL measurements, it is very common to deal with the normalized thermal lens induced phase shift, $\Theta=-\theta/P_{abs}$, which can be written as

$$\Theta=C\left(1-\eta_0\frac{\lambda_{exc}}{\langle\lambda_{em}\rangle}\right), \tag{5}$$

where $C=(\lambda_p K)^{-1}ds/dT$ is a constant independent on the particular pump wavelength. It depends only on the probe

beam wavelength through ds/dT, since refractive index, determining the ds/dT value, is strongly dependent on λ_p and also on wave polarization. As a consequence, in biaxial crystal such as NAB, C is expected to be somehow dependent on the polarization of the probe beam.

Then by adjusting the $I(t)$ transient curves to expression (1) it is possible to obtain the characteristic TL time (t_c) and so the value of the thermal conductivity and diffusivity (note that $t_c = w_e^2/4D$ and that $D = K/\rho \cdot c$). Furthermore, by the analysis of the transient curves obtained under different pump wavelengths it is also possible to determine the dependence of the TL induced probe beam phase shift on the pump wavelength (multi wavelength thermal lens measurements[5]). If a linear relation is obtained it is then possible, by fitting the experimental data to expression (5), to obtain the value of the metastable state quantum efficiency and the constant C. Since the value of the thermal conductivity has been already estimated, then the knowledge of constant C provides the temperature coefficient of the optical path length ($ds/dT = C\lambda_p K$).

The TL experiments were performed using the time-resolved mode mismatched configuration shown in detail elsewhere.[17–19] As a matter of fact, this configuration has proved to be the most sensitive.[18,19] For the determination of fluorescence quantum efficiency by multiwavelength TL measurements,[5] pump wavelength was varied by using different continuous wave laser sources: Ti:sapphire for 765, 810 and 876 nm pumping, a dye laser for 600 and 580 nm pumping, and an Ar^+ laser for 476, 514 and 528 nm pumping. In these experiments the pump power was always keep below, $\leqslant$10 mW, in order to determine the value of η_0, i.e., the value of quantum efficiency in absence of upconversion processes. As a probe beam we used a polarized He-Ne laser at 632.8 nm. More details of the experimental setup can be found elsewhere.[17–19]

B. Energy transfer upconversion

In the previous section we have dealt with the determination of the intrinsic fluorescence quantum efficiency of the $^4F_{3/2}$ metastable state, i.e., only taking into account radiative and nonradiative decays from this state (losses only by down-conversion). Nevertheless, in Nd^{3+} doped lasers under high or even moderate pumping intensities ETU processes can take place due to the high populations achieved in the departing laser level.[13,14,21] If ETU processes are considered, the dynamics of $^4F_{3/2}$ level can be described by

$$\frac{dN_e}{dt} = \frac{\sigma_{abs} I}{h\nu_{exc}} N_g - \frac{N_e}{\tau_F} - \gamma N_e^2, \tag{6}$$

where N_e is the metastable (excited) state population, N_g is the ground state ($^4I_{9/2}$) population, $N_t \approx N_e + N_g$ is the total Nd^{3+} ion population, σ_{abs} is the absorption cross-section for pump radiation, I is the pump intensity which is usually expressed in terms of the saturation parameter $S = I/I_s$ (the ratio between the pump intensity and the saturation intensity, $I_s = h\nu_{exc}/\sigma_{abs}\tau_F$), τ_F is the fluorescence lifetime of metastable state and $\gamma(\mathrm{cm}^3/\mathrm{s})$ is the upconversion parameter. In the very low pump regime, $\gamma N_e \ll \tau_F^{-1}$, the fluorescence decay rate (τ_F^{-1}) is given by the sum of the radiative (τ_{rad}^{-1}), multiphonon, and cross relaxation decay rates. For high pump intensities, the ETU mechanisms becomes relevant and results in an additional decay rate $W_{up} = \gamma N_e$. Since W_{up} increases with N_e, it does lead in general, to nonexponential fluorescence decay curves.

In the absence of ETU (very low pump power regime) the intrinsic fluorescence quantum efficiency of a given level is given by $\eta_0 = \tau_F/\tau_{rad}$ (i.e., the ratio between its radiative and total rates). As the pump rate increases, and consequently N_e as well, ETU becomes significant and the total decay rate can be written as $W_t = \tau_F^{-1} + \gamma N_e$. Therefore, since the fluorescence quantum efficiency is given by $\eta = W_{rad}/W_t$, it can be written as[22,23]

$$\eta = \frac{\eta_0}{1 + \beta n_e}, \tag{7}$$

where $n_e = N_e/N_t$ is the fraction of ions in the metastable state and $\beta = \gamma\tau_F N_t$ is a dimensionless parameter related to the strength of ETU processes. Equation (7) shows that as n_e is increased by the excitation power, η is reduced due to the term $1 + \beta n_e$ associated to ETU. According to Eq. (5), any dependence of the quantum efficiency on the pump power is expected to induce a nonlinear relation between the normalized TL induced phase shift and the pump power. Taking into account expression (7), Eq. (4) can be rewritten as

$$\Theta = C\left(1 - \frac{\eta_0}{1 + \beta n_e} \frac{\lambda_{exc}}{\langle \lambda_{em} \rangle}\right). \tag{8}$$

Therefore, by measuring Θ for different pump powers (i.e., different n_e values) it is possible to determine β and so the value of the upconversion parameter $\gamma(\gamma = \beta/\tau_F N_t)$.

For the determining the upconversion parameter we used the same set-up as for the intrinsic fluorescence quantum efficiency determination. In this case the pump wavelength was set to 810 nm by using the beam from the Ti:sapphire laser. Pump power was varied from few mW up to a maximum value of 200 mW being this a typical pump power for NAB end pumped lasers (laser thresholds of NAB crystals are usually of the order of 50 mW).[11]

III. RESULTS AND DISCUSSION

A. Thermal diffusivity and conductivity. Intrinsic fluorescence quantum efficiency

Figure 1 shows a typical TL transient signal for a π polarized probe beam. The excitation wavelength and power used in this case were 810 nm and 10 mW, respectively. The solid curve represents the best fit to expression (1). In this fitting, the parameters $m = 16$ and $V = 1.73$ are fixed in accordance to our particular experimental conditions. Similar curves and good agreements between experimental data and expression (1) have been found when different pump wavelengths and probe beam polarizations were used. The thermal conductivity and diffusivity values obtained from these curves are listed in Table I. The same parameters reported for other Nd^{3+} doped laser crystals are also included in Table I for the sake of comparison. By inspecting this table, it can be

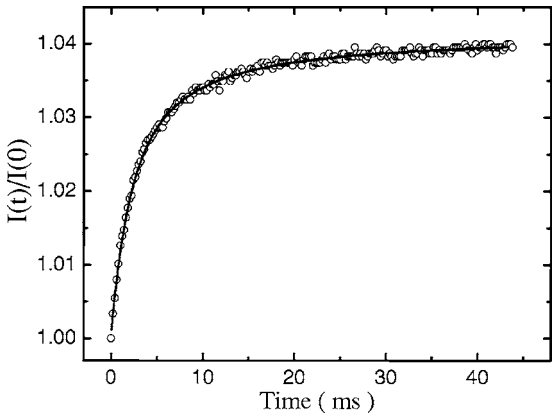

FIG. 1. Transient thermal lens signal for NAB sample with $P=10$ mW at $\lambda_{exc}=810$ nm. The solid line indicates the fitting where $\theta=-(0.0406\pm0.0001)$ and $t_c=(0.294\pm0.002)$ ms were obtained. For this transient the parameters fixed were $m=16$ and $V=1.73$.

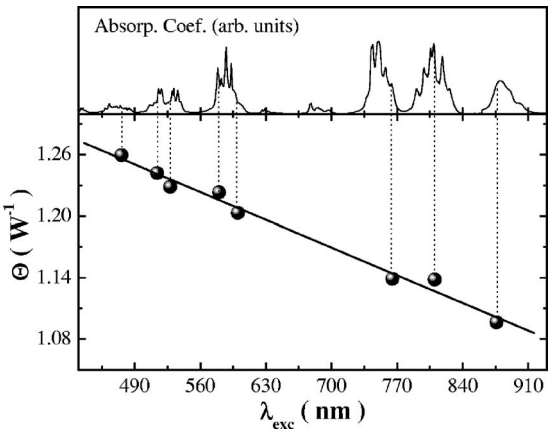

FIG. 2. Measured values of Θ as a function of the excitation beam wavelength. The inset shows the NAB absorption spectra with the used excitation wavelengths properly indicated.

observed that the thermal conductivity obtained for NAB is even higher than that previously reported for the $Nd:YVO_4$ laser system,[24,25] a widely studied gain medium for microchip cavities.

For the determination of the intrinsic fluorescence quantum efficiency, η_0, we have obtained the normalized TL induced phase shift, $\Theta=-\theta/P_{abs}$, for different pump wavelengths. In all the cases, low excitation powers were used in such a way that a linear dependence of θ versus the input power was obtained, indicating the absence of upconversion losses from the $^4F_{3/2}$ state. Results are shown in Fig. 2, together with the absorption spectrum of Nd^{3+} ions in NAB. As predicted by expression (5) a linear relation between Θ and the pump wavelength is observed (solid line shows the best fit to a linear relation). To obtain the value of η_0 from these data, it is necessary to know the average fluorescence wavelength from the $^4F_{3/2}$ metastable state. This has been calculated by using the previously reported "*branching ratio*" and the average emission wavelengths for each fluorescence channel departing from the metastable state (i.e., $^4F_{3/2}\rightarrow{}^4I_{9/2}$, $^4F_{3/2}\rightarrow{}^4I_{11/2}$, $^4F_{3/2}\rightarrow{}^4I_{13/2}$, and $^4F_{3/2}\rightarrow{}^4I_{15/2}$).[26] We have estimated an average fluorescence wavelength equal to $\langle\lambda_{em}\rangle=1.007$ μm. Using this value, together with the linear fit of experimental data of Fig. 2 we have obtained an intrinsic fluorescence quantum efficiency equal to 0.30 ± 0.04.

The η_0 value achieved by this multiwavelength method is no far from that determined by the Judd Ofelt theory, 0.18, for this crystal.[27] Indeed, this quantum efficiency is high when compared to that estimated for other Nd^{3+} stoichiometric crystals such as $NdPO_4$ or Nd_3BWO_9 ($\eta_0<0.05$).[9] As a matter of fact, the fluorescence lifetime of Nd^{3+} ions in NAB ($\tau_F\approx20$ μs) is more than one order of magnitude larger than those corresponding to these other stoichiometric crystals ($\tau_F\approx0.5$ μs).[28,29] Furthermore, this value is similar to that obtained for moderately Nd^{3+} doped (5 at. %)$YAl_3(BO_3)_4$ crystals as obtained by multiwavelength photoacoustic measurements ($\eta_0=0.26\pm0.05$) and by the Judd Ofelt theory ($\eta_0=0.18$).[30,31] It should be noted that relatively low fluorescence quantum efficiencies are characteristic of Nd^{3+} doped borate crystals as in these crystals a high multiphonon relaxation rate is favored because the energy gap from the metastable state to the lower level $^4I_{9/2}$ can be filled with about three of the highest energy phonons (~1360 cm^{-1} in NAB).[32] This high multiphonon relaxation

TABLE I. Thermo-optical properties of NAB and some relevant Nd-doped crystals.

Material	D (10^{-3} cm^2 s^{-1})	K (W m^{-1} K^{-1})	ds/dT (10^{-6} K^{-1})	Ref.
NAB	18.7±0.9	7.2±0.4	6.6±0.4∥c	This work
			9.4±0.4⊥c	
Nd:YAG	48.0	13.0	13.7	29 and 40–43
Nd:YAP	49.0	11.0	20∥c	41 and 44
			16.0⊥c	
NYAB		3.0 to 4.0	9.5	45
Nd:YLF	19.0	5.8∥c	18.0∥c	20 and 43
		7.2⊥c	20.0⊥c	
GSGG	23.4	6.0	19.75	43
(1%) $Nd:YVO_4$	48.0∥c	5.2∥c	15.4∥c	20 and 21
	44.0⊥c	4.8⊥c	12.7⊥c	

rate leads to reduced fluorescence quantum efficiencies. The anomalous nonvanishing quantum efficiency obtained for NAB crystals can be explained in terms of its stoichiometric character. Since Nd^{3+} ions are forced to constitute crystal lattice, the formation of Nd^{3+}-Nd^{3+} pairs or Nd^{3+} clusters, leading to short Nd^{3+}-Nd^{3+} distances and therefore to a strong luminescence quenching, is avoided.

Following the description given in Sec. II A and by using the linear fit of Fig. 2 together with the previously determined thermal conductivity, it is possible to calculate the ds/dT coefficient. Results are also listed in Table I together with those obtained for other Nd^{3+} doped laser crystals. As can be observed the ds/dT value of NAB is relatively small when compared for other Nd^{3+} doped laser crystals. This is of special relevance when dealing with a potential microchip laser material. In an unstable plane-plane cavity configuration (that corresponding to a microchip laser), the stability of the resonator is mainly provided by the pump induced thermal lens of the gain medium. It has been previously stated that when a TL with its corresponding focal length, $f_{TL}=(\pi w_e^2 K)/P_{abs}\varphi ds/dT$,[33] is induced in the gain medium, the plane-plane resonator becomes stable only if the cavity length, l_{cavity}, is smaller than f_{TL} (the stability criteria is then written as $f_{TL} \geqslant l_{cavity}$).[12,34] Since f_{TL} is proportional to $(ds/dT)^{-1}$, low values of ds/dT ensure large TL focal lengths and, therefore, large stability for a microchip cavity configuration.

B. Auger upconversion losses

In absence of ETU, Eq. (5) predicts that Θ (in a very low power regime, such as that of Sec. III A) should be independent of the excitation power. This independence has been observed in many experiments, including Nd^{3+} doped glasses.[19] However, in the high power regime Θ does not remain constant with the pump intensity (again, I is usually expressed in terms of the saturation parameter $S=I/I_s$), because ETU causes a nonlinear increase of the TL signal (θ) with increasing excitation power.[22,23,35] Figure 3 shows Θ as a function of the saturation parameter (S) corresponding to pump powers up to 200 mW, typical pump powers previously used in laser gain experiments on NAB crystals.[11] The obtained increment of Θ with S can be attributed to the increase of the fractional thermal loading (φ), which in turn is caused by the decrease of the fluorescence quantum efficiency with excitation intensity due to ETU.

The fit of Θ versus S experimental data (see Fig. 3) to expression (8), where $n_e(S)$ was obtained by solving the Eq. (6) in the steady state, provides the β paramenter. Then, taking into account that $\beta=\gamma\tau_F N_t$, the upconversion parameter, γ, can be experimentally determined. We have found that $\gamma_{TL}=30\times10^{-16}$ cm^3/s. This value will be next compared to that calculated from the microscopic description of ETU processes.

Analyzing the physical mechanisms involved in ETU, the upconversion processes could occur through two different energy transfer mechanisms: static transfer (Förster-Dexter "FD" model) and migration-assisted energy transfer (MAET).[36–39] In the first case, FD theory, the donor excitation is transferred to an acceptor directly. In the case of ETU processes this means that upconversion takes place only if in its vicinity there is another excited ion. The probability of this process is, therefore, strongly dependent on the density of excited ions (i.e., on the excitation intensity and on the ion concentration). In the second case, MAET, the excitation migrates over donors before it reaches an acceptor, from where energy can be transferred by a more efficient way. In this way the requirement of two excited ions to be close in the crystal lattice is not so restrictive as energy can migrate up to another excited ion is reached. Therefore, the migration mechanism causes an enhancement of the energy transfer to acceptors. These two mechanisms could be simultaneously contributing to the total upconversion parameter. According to this, the total upconversion rate is given by[13,24,40]

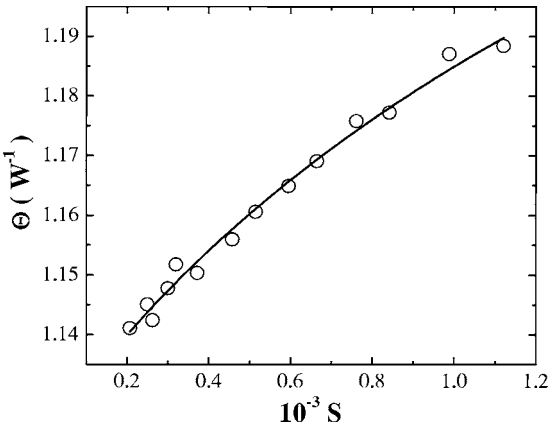

FIG. 3. TL signal amplitude normalized by the absorbed power (Θ) as a function of the excitation parameter S for $\lambda_{exc}=810$ nm.

$$W_{up}=\gamma N_e=(\gamma^{FD}+\gamma_{mig})N_e, \tag{9}$$

where

$$\gamma^{FD}=2\left(\frac{4}{3}\right)^2\pi^3(R_{Auger})^6\frac{N_e}{\tau_{rad}} \tag{10}$$

and γ_{mig} is the upconversion parameter in the presence of energy migration among donors. There are two mathematical models used to describe this parameter. One of them considers the energy migration as a diffusion process. This situation is assumed when the donor-acceptor interaction is stronger than the donor-donor interaction. This method was adopted by Yokota and Tanimoto (YT) who obtained[39,41,42]

$$\gamma_{mig}^{YT}=2\times0.676\left(\frac{8\pi^2}{3}\right)2^{1/4}(R_{Auger})^{3/2}(R_{mig})^{9/2}\frac{N_t-N_e}{\tau_{rad}}. \tag{11a}$$

The other is to describe the energy migration by the hoping model, which assumes that the excitation energy jumps among the donors until a donor-acceptor interaction occurs. This description is applied when donor-donor energy transfer is the dominant process. This hoping model was developed by Burstein who obtains the following expression for the upconversion parameter:[37,39,40]

$$\gamma_{mig}^{B} = 2\pi\left(\frac{2\pi}{3}\right)^{5/2}(R_{Auger})^3(R_{mig})^3\frac{N_t - N_e}{\tau_{rad}}. \quad (11b)$$

Note that a factor of two has been added to Eqs. (10), (11a), and (11b) to account for the indistinguishability of Nd excited states.[22,40] In these expressions R_{Auger} is the so-called critical radius for Auger upconversion and R_{mig} is the critical radius for the energy migration mechanism. These critical radii are related to the energy transfer microparameters $C_{DA}=C_{FD}$ and $C_{DD}=C_{mig}$ which are given by

$$C_{FD} = \frac{R_{Auger}^6}{\tau_{rad}} = \frac{3c}{8\pi^4 n^2}\int \sigma_{SE}(\lambda)\sigma_{ESA}(\lambda)d\lambda, \quad (12)$$

$$C_{mig} = \frac{R_{mig}^6}{\tau_{rad}} = \frac{3c}{8\pi^4 n^2}\int \sigma_{SE}(\lambda)\sigma_{GSA}(\lambda)d\lambda, \quad (13)$$

where σ_{SE}, σ_{ESA} and σ_{GSA} refer to the stimulated emission, excited-state absorption, and ground state absorption cross sections and n is the refractive index. The ground-state absorption spectrum has been obtained with the aid of a standard spectrometer. The stimulated emission cross section spectra has been derived from the emission spectra by using the well-known Fuchtbauer-Ladenburg formula. Finally, we have obtained the excited state cross section from the excited state excitation spectra after calibrating them with the help of Judd-Ofelt parameters. By introducing the obtained σ_{SE}, σ_{ESA} and σ_{GSA} spectra in expressions (12) and (13) we have obtained $C_{DD}=C_{mig}=9.0\times10^{-39}$ cm^6/s and $C_{DA}=C_{FD}=10\times10^{-38}$ cm^6/s. It should be noticed that our experiment was performed in the low excitation regime (S lower than 0.0012) then N_t-$N_g \approx N_t$. According to Eqs. (10) and (11), the FD mechanism should have negligible effect since, for the excitation energies used in this work, N_e is more than three orders of magnitude smaller than N_t. Additionally, using C_{DD} and C_{DA} in Eq. (11a), we obtain $\gamma_{mig}^{YT}=37\times10^{-16}$ cm^3/s. Indeed, the calculated value is quite close for the obtained by TL ($\gamma_{TL}=30\times10^{-16}$ cm^3/s). Consequently, we can state that in the range of pump intensities used in this work (coinciding with the typical pump intensities achieved in laser gain experiments) the main mechanism contributing to ETU processes in NAB is the migration assisted mechanism and that it can be properly described by considering donor-donor migration as a diffusion mechanism.

The obtained value for the upconversion parameter is relatively large compared to those found for laser crystals such as Nd:YAG (2.8×10^{-16} cm^3/s for sample doped with 1.38×10^{20} ions/cm^3 of Nd^{3+})[43] and Nd:YLF (1.9×10^{-16} cm^3/s for a sample with 1.7×10^{20} ions/cm^3 of Nd^{3+}).[22,43] Considering the high Nd^{3+} concentration in NAB crystal, γ can be still considered very low, because it is only ten times that of Nd:YAG, whereas the Nd concentration is 40 times. On the other hand, the loss-inducing parameter $N_c=\tau_F\gamma=6.0\times10^{-20}$ cm^3 for NAB is well small, considering the high Nd concentration of this crystal. N_c is usually called critical inversion density, since $W_{up}=\tau^{-1}$ when $N_e=N_c$. For Nd:YAG and Nd:YLF the N_c values are 6.4×10^{-20} and 9.9×10^{-20} cm^3, respectively.[22,43] The lower loss induced parameter is another outstanding feature of NAB crystals as laser gain media as larger values of $\tau_F\gamma$ causes a deterioration of laser performance under high pumping intensities as it occurs for Nd:YAG crystals.[21] The relatively low loss induced parameter ensures high conversion efficiencies even under high pumping intensities.

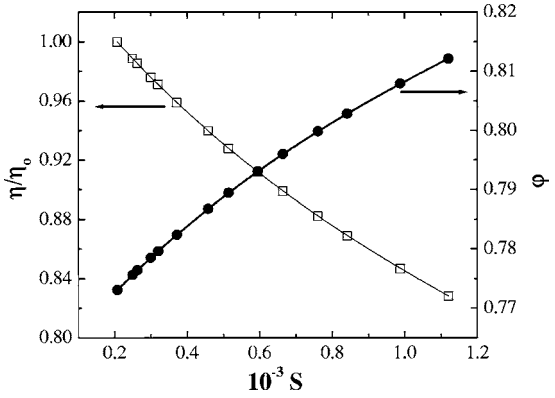

FIG. 4. Fluorescence quantum efficiency normalized (η/η_0) and fractional thermal loading (φ) as a function of the excitation parameter S for $\lambda_{exc}=810$ nm.

Finally, we have also used the data of Fig. 3 to elucidate on the effect of upconversion processes on the fluorescence quantum efficiency. In this sense Fig. 4 shows both the fluorescence quantum efficiency normalized to the intrinsic quantum efficiency (η/η_0) and the fractional thermal loading (φ) as a function of the excitation parameter S. From this figure, it is clear that the influence of ETU in the heat generation processes taking place in a strongly pumped NAB laser cannot be neglected. As a matter of fact, a reduction of $\sim$16% in the fluorescence quantum efficiency due to ETU has been found for a saturation parameter $S=0.001$. For this saturation parameter we have predict a slight enhancement of the thermal load of $\sim$5%. Therefore, when strongly pumped, any estimation of the thermal loading in NAB microchip laser should include the effect of ETU processes.

IV. SUMMARY AND CONCLUSIONS

In summary, we have experimentally determined the fluorescence quantum efficiency and the thermo-optical properties (D, K, and ds/dT) of the NAB microchip laser crystal by using the TL technique. The obtained value for the fluorescence quantum efficiency ($\eta\approx0.30$) is in reasonable agreement with those determined using the Judd-Ofelt formalism. We have concluded that the main mechanism limiting the fluorescence quantum efficiency is multiphonon relaxation rather than energy migration and fluorescence quenching caused by Nd^{3+}-Nd^{3+} interactions.

We have also demonstrated that the nonlinear dependence of the TL signal with excitation power can be used to study the energy-transfer upconversion in a highly doped crystal like NAB. As a photothermal technique, this method does not require any assumption about the fluorescence kinetics, which is usually a complex phenomenon. We have investigated the effect of upconversion losses on the fluorescence quantum efficiency of $^4F_{3/2}$ level. By comparing the experi-

mental value obtained for the upconversion parameter with that calculated on the basis of energy transfer microparameters, we have been able to determine that ETU processes in NAB are mainly caused by an energy migration assisted mechanism. The good agreement between the γ_{up} values obtained from TL and microparameters calculus, jointly with sensitive and accurate of the TL technique, indicate that the TL spectrometry is a valuable method to determine upconversion parameters. Another advantage of the TL technique compared to transient measurements is the use of a cw pump source instead of a pulsed one. This is an advantage because such a procedure reduces the errors involved on the determination of radius and pump power of the excitation beam, which are the most important experimental variables to be known for an accurate experiment.

Finally, we have concluded that both the fluorescence quantum efficiency and the fractional thermal loading are, as a consequence of ETU processes, strongly dependent on the pumping intensity. Consequently, ETU constitutes a nonnegligible heating channel which should be included in future modeling of pump induced thermal loading in NAB microchip lasers.

ACKNOWLEDGMENTS

The authors are thankful to CNPq and FAPESP for the financial support of this work. This work has been supported by the Comunidad Autónoma de Madrid (projects 07N/0020/2002 and GR/MAT/0110/2004) and by Spanish Ministerio de Ciencia y Tecnología (MAT2004-03347). Authors thank the group of Professor Luo Zundu (Fuzhou, China) for providing us the NAB sample. One of the authors (T.C.) thanks to Dr. S. L. Oliveira for discussions.

*Electronic address: carlosjs@if.sc.usp.br

[1] J. J. Zayhowski and C. D. Dill III, Opt. Lett. **19**, 1427 (1994).
[2] G. J. Spühler, R. Paschotta, R. Fluck, B. Braun, M. Moser, G. Zhang, E. Gini, and U. Keller, J. Opt. Soc. Am. B **16**, 376 (1999).
[3] V. Lupei and A. Lupei, Phys. Rev. B **61**, 8087 (2000).
[4] D. Jaque, J. J. Romero, U. Caldiño, and J. García Solé, J. Appl. Phys. **86**, 6627 (1999).
[5] S. M. Lima, A. A. Andrade, R. Lebullenger, A. C. Hernandes, T. Catunda, and M. L. Baesso, Appl. Phys. Lett. **78**, 3220 (2001).
[6] I. Iparraguirre, R. Balda, M. Boda, M. Al Saleh, and J. Fernandez, J. Opt. Soc. Am. B **19**, 2911 (2002).
[7] V. Ostroumov, T. Jensen, J.-P. Meyn, G. Huber, and M. A. Noginov, J. Opt. Soc. Am. B **15**, 1052 (1998).
[8] M. B. Danailov, A. A. Demidovich, A. N. Kuzmin, O. V. Kuzmin, and V. L. Hait, Appl. Phys. B **73**, 671 (2001).
[9] A. Majchrowski, E. Michalski, and A. Brenier, J. Cryst. Growth **247**, 467 (2003).
[10] S. R. Chinn and H. Y.-P. Hong, Opt. Commun. **15**, 345 (1975).
[11] Z. D. Luo, Y. D. Huang, M. Montes, and D. Jaque, Appl. Phys. Lett. **85**, 715 (2004).
[12] M. Montes, D. Jaque, Z. D. Luo, and Y. D. Huang, Opt. Lett. **30**, 397 (2005).
[13] J. L. Doualan, C. Maunier, D. Descamps, J. Landais, and R. Moncorgé, Phys. Rev. B **62**, 4459 (2000) (and references therein).
[14] M. Pollnau, P. J. Hardman, M. A. Kern, W. A. Clarkson, and D. C. Hanna, Phys. Rev. B **58**, 16076 (1998).
[15] D. Jaque, O. Enguita, Z. D. Luo, J. García Solé, and U. Caldiño, Opt. Mater. (Amsterdam, Neth.) **25**, 9 (2004).
[16] S. J. Sheldon, L. V. Knight, and J. M. Thorne, Appl. Opt. **21**, 1663 (1982).
[17] M. L. Baesso, J. Shen, and R. D. Snook, J. Appl. Phys. **75**, 3732 (1994).
[18] S. M. Lima, J. A. Sampaio, T. Catunda, A. C. Bento, L. C. M. Miranda, and M. L. Baesso, J. Non-Cryst. Solids **273**, 215 (2000).
[19] M. L. Baesso, A. C. Bento, A. A. Andrade, J. A. Sampaio, E. Pecoraro, L. A. O. Nunes, T. Catunda, and S. Gama, Phys. Rev. B **57**, 10545 (1998).
[20] In the case where there is only one emitting channel. In Nd-doped systems normally all radiative transitions are basically from the $^4F_{3/2}$ metastable state.
[21] T. Chuang and H. Verdun, IEEE J. Quantum Electron. **32**, 79 (1996).
[22] C. Jacinto, S. L. Oliveira, T. Catunda, A. A. Andrade, J. D. Myers, and M. J. Myers, Opt. Express **13**, 2040 (2005).
[23] V. Pilla, T. Catunda, H. P. Jensen, and A. Cassanho, Opt. Lett. **28**, 239 (2003).
[24] A. A. Andrade, T. Catunda, I. Bodnar, J. Mura, and M. L. Baesso, Rev. Sci. Instrum. **74**, 877 (2003).
[25] VLOC, http://www.vloc.com/ncatalog/vloccat.pdf
[26] D. Jaque, O. Enguita, U. Caldiño, G. M. O. Ramirez, J. García Solé, C. Zaldo, J. E. Muñoz-Santiuste, A. D. Jiang, and Z. D. Luo, J. Appl. Phys. **90**, 561 (2001).
[27] X. Chen, Z. Luo, D. Jaque, J. J. Romero, J. Garcia Solé, Y. Huang, A. Jiang, and C. Tu, J. Phys.: Condens. Matter **13**, 1171 (2001).
[28] D. Jaque, J. García Solé, L. Macalik, J. Hanuza, and A. Majchrowski, Appl. Phys. Lett. **86**, 011920 (2005).
[29] A. Ródenas, D. Jaque, J. García Solé, A. Speghini, E. Cavilla, and M. Bettinelli (unpublished).
[30] D. Jaque, J. Capmany, Z. D. Luo, and J. García Solé, J. Phys.: Condens. Matter **12**, 9715 (1997).
[31] D. Jaque, J. A. Muñoz, F. Cussó, and J. García Solé, J. Phys.: Condens. Matter **10**, 7901 (1998).
[32] H. Kim, Chin. Phys. Lett. **5**, 1 (1988).
[33] C. Jacinto, A. A. Andrade, T. Catunda, S. M. Lima, and M. L. Baesso, Appl. Phys. Lett. **86**, 034104 (2005).
[34] M. E. Innocenzi, H. T. Yura, C. L. Fincher, and R. A. Fields, Appl. Phys. Lett. **56**, 1831 (1990).
[35] P. J. Hardman, W. A. Clarkson, G. J. Friel, M. Pollnau, and D. C. Hanna, IEEE J. Quantum Electron. **35**, 647 (1999).
[36] Th. Förster, Z. Naturforsch. A **4**, 321 (1949).
[37] A. I. Burstein, Zh. Eksp. Teor. Fiz. **62**, 1699 (1972) [Sov. Phys. JETP **35**, 882 (1972)].

[38] M. Inokuti and F. Hirayama, J. Chem. Phys. **43**, 1978 (1965).
[39] R. C. Powell, *Physics of Solid-State Laser Materials* (American Institute of Physics, New York, 1998).
[40] S. A. Payne, G. D. Wilke, L. K. Smith, and W. F. Krupke, Opt. Commun. **111**, 263 (1994).
[41] M. Yokota and F. Tanimoto, J. Phys. Soc. Jpn. **22**, 779 (1967).
[42] I. R. Martin, V. D. Rodriguez, U. R. Rodríguez-Mendoza, V. Lavin, E. Montoya, and D. Jaque, J. Chem. Phys. **111**, 1191 (1999).
[43] Y. Guyot, H. Manaa, J. Y. Rivoire, R. Moncorgé, N. Garnier, E. Descroix, M. Bon, and P. Laporte, Phys. Rev. B **51**, 784 (1995).
[44] W. Koerchner, *Solid-State Laser Engineering* (Springer, New York, 1988).
[45] A. A. Kaminskii, *Laser Crystals* (Springer, Berlin, 1986).